ADVANCED MATERIALS INTERFACES
www.advmatinterfaces.de

Stratified Polymer Grafts: Synthesis and Characterization of Layered 'Brush' and 'Gel' Structures

Ang Li, Shivaprakash N. Ramakrishna, Prathima C. Nalam, Edmondo M. Benetti, and Nicholas D. Spencer**

The development of surface coatings with well-defined architecture is of particular interest in several disciplines, notably in biomaterials. Bio-organic layers on different length-scales, featuring variable composition, structure and modulus have been observed in several biological systems, such as human cartilage, mammalian skin and the nacre of oyster shells.[1–3] These complex systems often consist of mechanically graded structures that resist and respond to external normal and shear forces, and therefore protect underlying tissues from incurring any damage. As an example, the human epidermis consists of keratinizing epithelial cells—an elastic layer with low modulus—buried under a layer of dead cells, the *stratum corneum*, with higher modulus. The stratified epithelium thus acts as the body's major barrier against abrasion and inhospitable environments.[4,5]

In order to mimic mechanically useful structures found in nature, materials scientists have been made numerous efforts to fabricate coatings with discontinuous mechanical properties at pre-determined depths in a single multilayered architecture. These materials, unlike homogenous films, have been shown to successfully redistribute contact stresses at the interface and to resist failure-inducing contact deformations.[6,7] Progress has also been made in fabricating graded morphologies of organic/inorganic nanocomposites, thereby mimicking the approach of natural counterparts, to obtain coatings with higher toughness and modulus.[8] Despite all these efforts, the fabrication of a full-organic, polymer-based coating architecture featuring nanoscale variations of properties still represents a challenging task in polymer and materials science.

Dr. A. Li,[+] Dr. S. N. Ramakrishna, Dr. P. C. Nalam,[++] Dr. E. M. Benetti, Prof. N. D. Spencer
Laboratory for Surface Science and Technology
Department of Materials, ETH Zurich
Wolfgang-Pauli-Strasse 10, HCI H 523,
8093, Zurich, Switzerland
E-Mail: edmondo.benetti@mat.ethz.ch;
nspencer@ethz.ch

Dr. E. M. Benetti
Department of Materials Science and Technology of Polymers
MESA+ Institute for Nanotechnology
University of Twente
P.O. Box 217, 7500, AE Enschede, The Netherlands

[+]Present address: Mettler-Toledo AG, Process Analytics, Im Hackacker 15, 8902, Urdorf, Switzerland

[++]Present address: Department of Mechanical Engineering and Applied Mechanics, University of Pennsylvania, 220 S. 33rd Street, Philadelphia, PA 19104, USA

DOI: 10.1002/admi.201300007

The development of surface-initiated polymerization (SIP) techniques[9] has provided a promising path towards the stepwise fabrication of stratified polymer films. To this end, controlled-radical SIP methods incorporating sequential polymerization processes can be applied.[10] With the exception of the pioneering work of Tsukruk et al.,[11] which introduced prototypes of stratified polymeric films, few such investigations have been reported. Moreover, the full characterization of stratified films, i.e. the physical and chemical analysis of the film properties at different depths (for each stratum), on the supporting substrate certainly represents a challenging experimental task. Although real-space analytical techniques, such as atomic force microscopy (AFM), enable access to surface properties in two dimensions, determination of physical properties in the third dimension (from surface to bulk) can be more readily achieved by reciprocal-space-based techniques, such as grazing-incidence, small-angle scattering (GISAS), or X-ray and neutron reflectivity—these methods are, at present, among the few that could determine the density profile of materials perpendicular to the sample surface. However, probing the vertical architecture of polymeric nanofilms with such techniques normally requires complex contrast-enhancing methods (isotopic labeling), which restricts their feasibility.[12]

Aiming at the fabrication of layered, surface-grafted polymeric films featuring graded physical properties, we report the synthesis by sequentially re-initiated SIP and subsequent characterization of stratified polyacrylamide (PAAm) films. Structural characterization was carried out by a combination of AFM-based nano-mechanical testing and lateral force microscopy (LFM). Two-layer films comprising either a 'free' polymer brush supporting a crosslinked brush-hydrogel (which we have previously defined as a 'brush-gel'[13] but will refer to henceforth as 'gel' for the sake of simplicity), or, alternatively, a gel supporting a 'free' brush were synthesized by sequential photoiniferter-mediated SIP (**Scheme 1**).[14] The inclusion of a determined amount of crosslinker at specified depths within these layers (demonstrated by ellipsometry, Fourier transform infrared spectroscopy FTIR, and LFM) allowed precise tuning of both interfacial and bulk film properties. In particular the mechanical and tribological characteristics of the films were investigated by measuring indentation profiles, pull-off and friction forces by means of colloidal-probe microscopy. These techniques provided a comprehensive characterization of the films and additionally clarified the re-initiation mechanisms and film morphology as a function of the polymerization conditions during the sequential photo-grafting steps. Along with the novel fabrication strategy proposed here, the mechanical and tribological study of stratified films has yielded a new

ADVANCED MATERIALS INTERFACES
www.advmatinterfaces.de

www.MaterialsViews.com

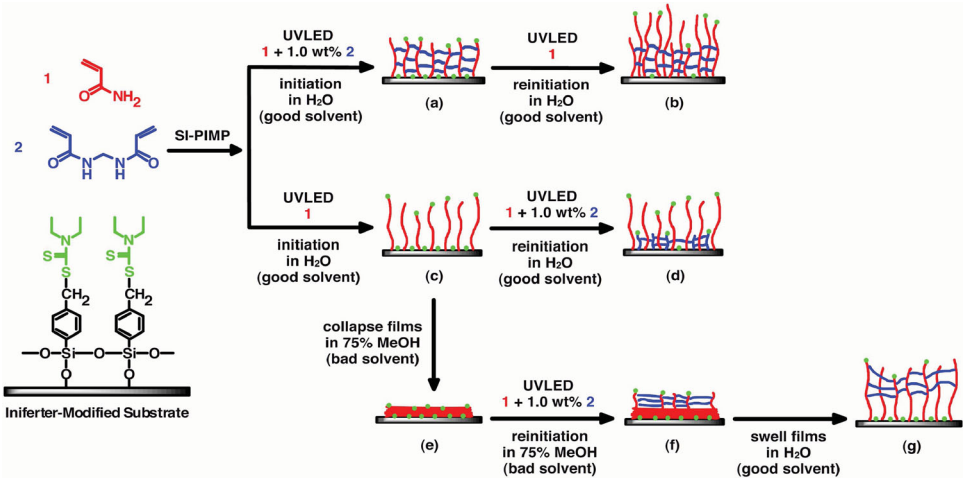

Scheme 1. Synthetic route to stratified PAAm films through sequential photoiniferter-mediated SIP. The stratified films in the text are represented as PAAm-a-b_c; the value of 'a' or 'b' indicates the wt% of crosslinker in the feed used during synthesis of the corresponding layer; subscript 'c' indicates the solvent used during reinitiation: water or 75% aqueous methanol solution. (a) PAAm-1 in water; (b) PAAm-1–0 in water; (c) PAAm-0 in water; (d) PAAm-0–1_{water} in water; (e) PAAm-0 in 75% aqueous methanol solution; (f) PAAm-0–$1_{methanol}$ in 75% aqueous methanol solution; (g) PAAm-0–$1_{methanol}$ in water.

understanding of the structure-dependent frictional response of polymeric films when studied at the nanoscale.

The stratified PAAm films were synthesized by sequential photoiniferter-mediated SIP as depicted in Scheme 1. Homogenous PAAm gels and brushes, denoted PAAm-1 and PAAm-0, respectively, were first photo-grafted from initiator-modified silicon substrates as previously described (see Scheme 1a,c, and Experimental Section for details).[14] For the synthesis of stratified gel-brush films (defined as PAAm-1–0), PAAm-1 was reinitiated by a UV-LED in the presence of an aqueous solution of acrylamide (AAm). This led to the layered PAAm-1–0 structure. The fabrication of brush-gel stratified films started from the previously synthesized PAAm-0 brush, but the final film architecture was found to be dependent on the medium used during reinitiation to produce the second (gel) layer: acrylamide/bisacrylamide (AAm/bisAAm) mixtures were either irradiated in pure water—a good solvent for the starting PAAm-0 brush layer (Scheme 1d, to yield PAAm-0–1_{water})—or in 75% methanol mixtures, which is a bad solvent for PAAm-0 brush (Scheme 1f,g, where the preparation of PAAm-0–$1_{methanol}$ is depicted). The characteristics of each layered structure resulting from the use of the two different solvents could be clarified by a combination of compositional, nano-mechanical and nano-tribological analysis on the films.

In order to chemically characterize the grafted PAAm films, FTIR measurements were performed on both homogeneous and stratified films. As shown in Figure S1 (Supporting Information), all FT-IR spectra showed similar profiles, indicating an almost constant chemical composition throughout the films.[14] Both amide I and amide II bands from AAm and bisAAm were found between 1480 and 1800 cm^{-1}. The appearance of a clear band at 1520 cm^{-1}, characteristic of the amide II band of bisAAm (highlighted by arrows), indicated the presence of crosslinker in the pure gel PAAm-1 (trace a in Figure S1) and in the layered PAAm-1–0 and PAAm-0–1 (traces b, d, and e in Figure S1). In these last two cases the relative intensity of amide II decreased following re-initiation from PAAm-1 to PAAm-1–0 (spectra a and b in Figure S1) and increased following the second photo-grafting step from PAAm-0 to PAAm-0–1 (Spectra c, d, and e in Figure S1).

Ellipsometry was used to determine the dry thickness of the films following sequential SIP (see the Experimental Section for details) and to establish the successful grafting of homogeneous and stratified PAAm layers featuring different architectures. In the case of PAAm-0 and PAAm-1, average dry thicknesses of 65 ± 5 and 185 ± 10 nm, respectively, were obtained following 30 min of irradiation. Re-initiation from homogeneous layers was evidenced by a significant increase in the ellipsometric thickness of the films. The stratified films studied—PAAm-1–0, PAAm-0–$1_{methanol}$ and PAAm-0–1_{water}—showed average thicknesses for each layer of 185–38, 65–135 and 39–53 nm, respectively (where the each pair of values refers to the underlayer and the surface layer, respectively). Thus, chain re-initiation by photoiniferter-mediated SIP was observed for all the stratified films prepared, confirming the effectiveness of this method for the fabrication of multi-layer brush structures.

Surface morphologies of the films were studied by tapping-mode AFM in an aqueous environment. Topography images in Figure S2 (Supporting Information) showed higher roughness for the PAAm-1 gel (Figure S2a, where the RMS was calculated as 5.5 ± 2 nm) in comparison to the linear polymer brush films PAAm-0 (Figure S2c, where RMS was calculated as 0.8 ± 0.2 nm). This phenomenon was reported in our previous studies[14] and appears to be due to a clustering of the crosslinked chains during synthesis. Re-initiation from homogenous PAAm-1 to form stratified PAAm-1–0 produced a decrease of surface roughness by 91% (Figure S2b where RMS was calculated as 0.5 ± 0.2 nm). In contrast, re-initiation from PAAm-0 films to form stratified PAAm-0–$1_{methanol}$ resulted in an increase of interfacial roughness that reached a RMS of 4.6 nm ± 1 (Figure S2d). This was presumably due to the formation of a crosslinked gel layer supported by PAAm-0.

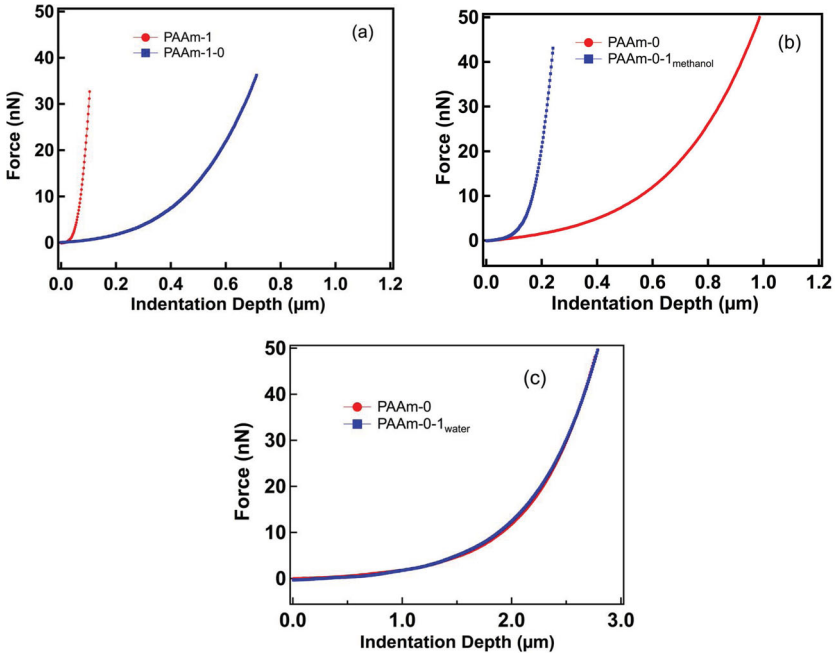

Figure 1. Indentation force curves of homogeneous and stratified PAAm films measured by CPM (spring constant: 1.28 N/m, radius of silica probe: 9.1 μm) in water. Dry mass of polymer films on silicon substrate: (a) PAAm-1: 148 mg/m^2, PAAm-1–0: 148–30 mg/m^2, (b) PAAm-0: 52 mg/m^2, PAAm-0–1$_{methanol}$: 52–108 mg/m^2. Indentation force curves of PAAm-0 and PAAm-0–1$_{water}$ films measured by CPM (spring constant: 0.51 N/m, radius of silica probe: 8.7 μm) in water. Dry mass of polymer films on silicon substrate: (c) PAAm-0: 31 mg/m^2, PAAm-0–1$_{water}$: 31–42 mg/m^2.

However, PAAm-0–1$_{water}$ did not show any morphological difference from PAAm-0 after re-initiation.

The mechanical properties of the different PAAm films were investigated by colloidal-probe microscopy (CPM) in an aqueous environment. The aim was to confirm the structure of the different samples and to verify the polymer architecture present at the interface following re-initiation. Force-vs.-indentation-depth plots for homogeneous and stratified films are reported in **Figure 1**. PAAm-1 gels displayed the highest values of Young's modulus (E) of 574 ± 35 kPa, while the highly swollen PAAm-0 showed E = 17 ± 3 kPa.[14] The successful formation of a brush layer on PAAm-1–0 by re-initiation from PAAm-1 was corroborated by the gentler indentation profiles for PAAm-1–0, resulting in a modulus of E = 20.8 ± 5.1 kPa (Figure 1a).

The brush-gel stratified layers, in contrast, displayed different nano-mechanical responses following re-initiation from PAAm-0, as a function of the quality of the solvent used for the second photo-grafting step. Re-initiation in an aqueous environment (to PAAm-0–1$_{water}$) unexpectedly produced a film showing very similar indentation profiles to the starting PAAm-0 (Figure 1c) with very similar E values of 6 ± 2 kPa for PAAm-0 and PAAm-0–1$_{water}$. When the second photo-grafting step was conducted instead in 75% methanolic solution, the corresponding layered PAAm-0–1$_{methanol}$ showed a stiffer interface, more characteristic of a gel structure, with E = 322 ± 17 kPa (Figure 1b). The significant shift of the indentation curve towards lower indentation depths implied that a degree of film shrinkage and stiffening had taken place, presumably caused by crosslinking between PAAm chains covering the PAAm brush underlayer. However, the indentation profiles for PAAm-0 and the corresponding PAAm-0–1$_{water}$ almost overlapped (Figure 1c) indicating that no detectable change in either the mechanical or the swelling properties of the top layer of PAAm-0–1$_{water}$ had occurred following re-initiation. Nevertheless, PAAm-0–1$_{water}$ showed a clear increase in ellipsometric dry thickness following the second SIP step (53 nm corresponding to 42 mg/m^2). Furthermore, FTIR spectroscopy of PAAm-0–1$_{water}$ films confirmed the successful incorporation of crosslinker upon re-initiation, as shown in Figure S1e. We can thus conclude that the re-initiation process, when performed in a good solvent for the PAAm-0 film, largely takes place within the brush film, presumably in the proximity of the substrate: initiator monolayers on SiO_x have previously been reported to show very low grafting efficiencies,[15] and thus the majority of iniferter groups remain potentially active at the substrate surface, below the brush. The significant swelling of PAAm brushes in pure water (previously measured as Q = 26)[14,16] allows a rapid diffusion of monomer species (AAm and bisAAm) through the brush, consequently exposing these molecules to the iniferter-rich monolayer. Unlike this initiator monolayer, the interface between the brush and a good solvent provides a relatively low concentration of iniferter chain-ends. Thus, reinitiation performed under these solvent conditions on the one hand causes a mass increase and a vertical expansion of the whole film (mainly due to mass increase close to the substrate) while, on the other hand, not substantially influencing the composition and the film structure at the interfacial layer to the bulk solvent. In support of this model, it should be noted that several past reports have demonstrated the sequential grafting of two different polymers in unselective solvents as an effective means to produce mixed brushes (rather than block-copolymers).[17–21] This strategy exploits the unreacted initiator at the surface and monomer species diffusing through the already formed film when exposed to sequential SIP.

Re-initiation of PAAm-0 under bad solvent conditions to produce PAAm-0–1$_{methanol}$ resulted in a brush-gel architecture. In this case, the effective fabrication of the desired layered film can be explained considering the distribution of reactive chain-ends as a function of different solvent qualities. The maximum in this distribution is to be found *within* the brush film, when this is immersed in a good solvent under equilibrium conditions.[22] In contrast, in a bad solvent the maximum probability of finding chain ends lies near the film's interface with the bulk (bad) solvent.[23–28] Thus, when re-initiation is carried out in a bad solvent, the strongly collapsed, substrate-tethered brush both protects the underlying substrate from monomer diffusion, and concentrates its reactive chain ends at the top

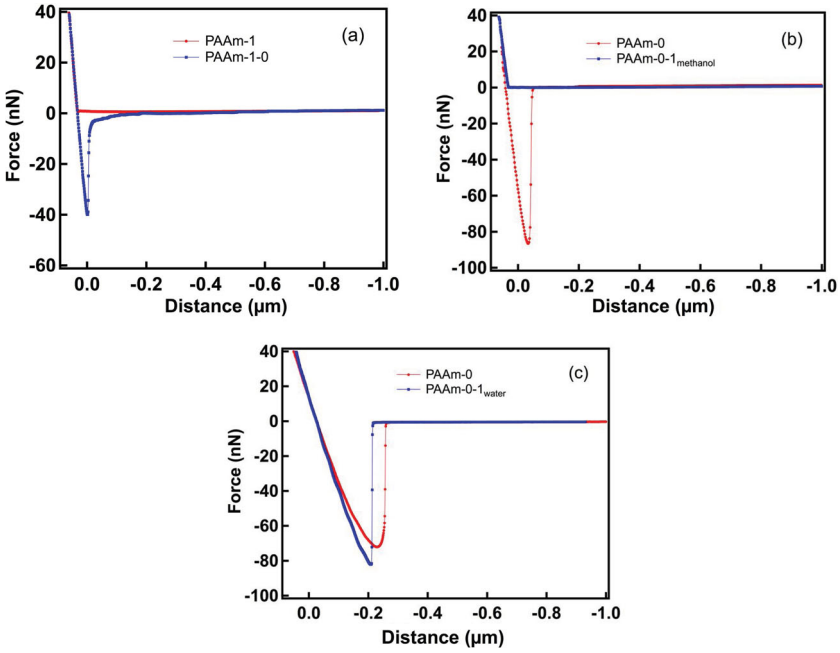

Figure 2. Pull-off forces of homogeneous and stratified PAAm films measured by CPM (spring constant: 1.28 N/m, radius of silica probe: 9.1 μm) in 75% aqueous methanol solution (only retracting curves are shown). Dry mass of polymer films on silicon substrate: (a) PAAm-1: 148 mg/m^2, PAAm-1–0: 148–30 mg/m^2, (b) PAAm-0: 52 mg/m^2, PAAm-0–1$_{methanol}$: 52–108 mg/m^2, (c) Pull-off forces measured by CPM (spring constant: 0.51 N/m, radius of silica probe: 8.7 μm) in aqueous methanol solution (volume fraction of methanol: 75%). Dry mass of polymer films on silicon substrate: PAAm-0: 31 mg/m^2, PAAm-0–1$_{water}$: 31–42 mg/m^2.

interface for re-initiation (as depicted in Scheme 1e,f). By means of this fabrication strategy, layered films with a brush-gel structures could thus be successfully obtained.

In addition to AFM nano-indentation, pull-off-force measurements were carried out, in order to determine the different polymer architectures exposed at the interface. As has previously been demonstrated,[29] brushes showed significantly higher adhesion when compared to grafted gels in 75% aqueous methanol solution. In **Figure 2**a, the very small pull-off forces (0.5 ± 0.1 nN) on PAAm-1 films indicated the presence of crosslinked chains at the interface. Further grafting of a brush layer on top of the gel subsequently resulted in a two-order-of-magnitude increase in pull-off force up to 40 ± 2 nN (Figure 2a), confirming the presence of dangling chains (brushes) at the interface of PAAm-1–0. In a similar manner, PAAm-0 films showed a very high pull-off force (85 ± 4 nN), typical for a brush near its (solvent-induced) glass transition. PAAm-0–1 films showed different adhesion properties as a function of the solvent quality employed during re-initiation, confirming the different structures obtained. Specifically, PAAm-0–1$_{methanol}$ was characterized by very small pull-off forces (0.3 ± 0.1 nN) indicating the successful formation of a well-defined brush-gel structure. A comparable reduction of adhesion was *not* found in the case of PAAm-0–1$_{water}$ (Figure 2c), which displayed very similar pull-off force to the corresponding PAAm-0 (72 ± 0.7 and 70 ± 10 nN, respectively). Thus, this result is consistent with the idea that the re-initiation process in pure water preferentially occurred at the residual iniferter monolayer rather than influencing the structure of the film at the outer interface.

Initiation efficiency, the presence of residual, unreacted initiator at the substrate surface, the distribution of dormant chain ends, and monomer diffusion through preformed brush layers were thus all found to be decisive parameters for sequential SIP and the efficient fabrication of stratified films. The first two factors rely on the photo-reactivity of the iniferter moieties and the irradiation intensity, parameters that are both considered as being constant during the re-initiation process. The last two parameters could be specifically adjusted by varying solvent quality, in order to guarantee the sequential preparation of well-defined grafted architectures.

It has also to be mentioned that monomer diffusion presumably also affected the gel-brush films in PAAm-1–0 but without substantially influencing the final stratified polymer architecture. In this case the starting PAAm-1 gel swollen in water presented an average mesh size of 3.3 ± 0.1 nm (see the Supporting Information), which would not have provided a significant steric barrier for monomer diffusion (Kuhn length of acrylamide: 0.3 nm).[30] Thus the swollen gel underlayer could not have completely prevented monomers from accessing the residual iniferter on the substrate. Re-initiation in this case occurred both at dormant chain-ends and at the substrate. Nevertheless, reinitiated chains were able to extend from the grafted gel layer into the bulk solvent, constituting the desired gel-brush structure.

Given the differences in both mechanical and adhesion properties of the studied PAAm films, we further investigated the nano-tribological characteristics of each film by LFM. The different polymer architectures exposed at the film's outer surface also influenced the frictional behavior of the films, thus providing additional insight into the structure of both homogeneous and layered films. **Figure 3**a,b depict the friction traces acquired for all the PAAm films. Over a sliding distance of 1 μm, both PAAm-0 (green curve) and PAAm-1–0 (blue curve) showed tilted friction loops with a small hysteresis. Due to the high water content and compliancy of the PAAm brush, we assumed that this particular friction behavior was due largely to lateral tilting of brush chains, the swollen chains being sufficiently long that true, steady-state sliding was never attained over the given 1 μm sliding distance.[31] Lateral tilting of the brushes due to the initial shear force from the probe is also consistent with our recent study,[32] in which we observed a surprisingly long time constant for conformational recovery following compression. This phenomenon was particularly marked for long chains and dilute brushes, as is the case for highly swollen and compliant PAAm grafts. Thus PAAm chains likely remain tilted in the trace direction for the duration of the experiment and give rise to the characteristic asymmetric friction loop as observed in Figure 3.[33]

In marked contrast, the crosslinked PAAm-1 (red curve) showed a friction trace with a stable sliding force (horizontal

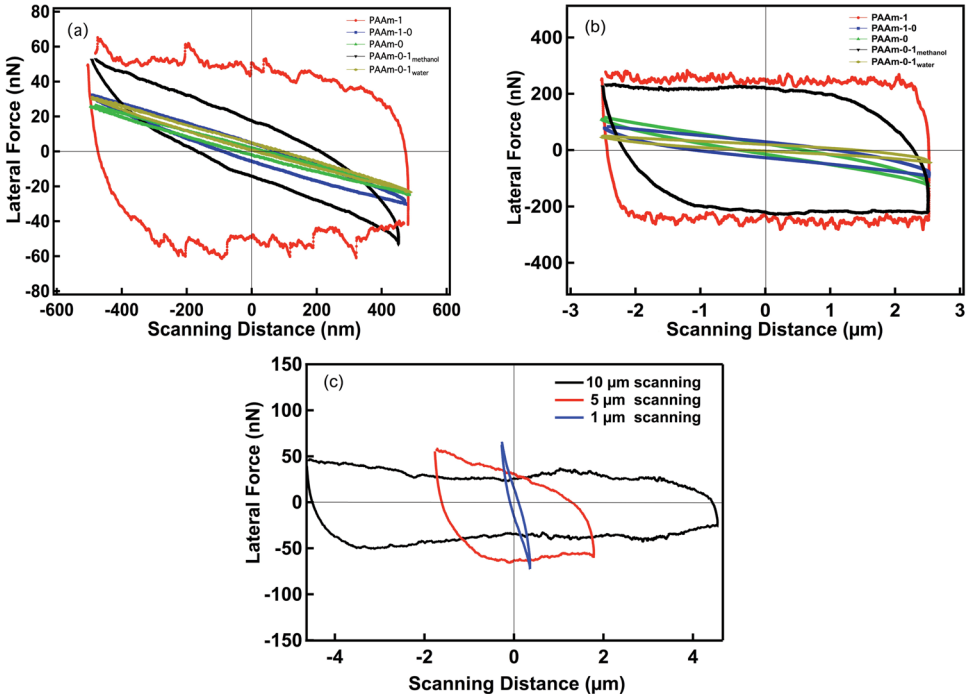

Figure 3. Representative friction loops of homogeneous and stratified PAAm films measured by CPM (spring constant: 1.28 N/m, radius of silica probe: 9.1 μm) in water at a load of 251 nN. Dry mass of polymer films on silicon substrate: PAAm-1: 148 mg/m^2, PAAm-1–0: 148–30 mg/m^2, PAAm-0: 52 mg/m^2, PAAm-0–1$_{methanol}$: 52–108 mg/m^2, PAAm-0: 31 mg/m^2, PAAm-0–1$_{water}$: 31–42 mg/m^2. (a) scanning distance: 1 μm, scan rate: 1 Hz; (b) scanning distance: 5 μm, scan rate: 1 Hz; (c) comparison of different scanning distances at same scanning speed (2 μm/s) and applied load (80 nN) for PAAm-0–1$_{methanol}$: 52–108 mg/m^2.

part in the loop) after overcoming an initial static friction (vertical part in the loop). The observed higher friction compared to PAAm 'free' brushes was due to the energy dissipation within the crosslinked network of chains at the top surface.[14] We further applied LFM on stratified PAAm-0–1$_{methanol}$ (black curve in Figure 3a), which, surprisingly showed a brush-like friction trace over 1 μm. This phenomenon was presumably due to the short sliding distance prior to direction reversal, which was insufficient to lead to steady-state sliding contact between the counter surface and the top surface of the film. Thus, static friction at the gel surface of PAAm0–1$_{methanol}$ dominated the tribological behavior for short sliding and the frictional properties were exclusively determined by the bending back and forth of the soft, swollen brush underlayer. This observation was confirmed by increasing the sliding distance to 5 μm, while maintaining the load constant (Figure 3b). In this case, PAAm-1, PAAm-0 and PAAm-1–0 films showed similar friction loops to those seen in the 1 μm scan case, while the stratified PAAm-0–1$_{methanol}$ displayed a transition from brush-like behavior at 1 μm (Figure 3a) to a gel-like trace at 5 μm (Figure 3b). Above a certain sliding-distance threshold (approximately 1.5 μm, which is comparable to the swollen extension of PAAm-0 underlayer) the static friction on the gel could be overcome by the spring force of the bent brush underlayer. The difference in lateral forces measured at 1 μm and 5 μm is related to the different scan speeds,[34] since the scanning frequency is maintained constant while the scan distance is varied. Figure 3c compares three different scanning distances at the same scan speed (and applied load) for PAAm-0–1$_{methanol}$, clearly showing the transition in friction-loop shape with scan distance.

Referring back to the stratum corneum/epidermis analogy given at the outset of this paper, this behavior is similar to that encountered when a dry finger is pressed upon and then moved laterally over fleshy parts of the body, such as the forearm. At first a distortion of the (sub-surface) epidermis occurs, but after a certain sliding distance, sliding begins over the skin.

The sliding mechanisms of PAAm-0–1$_{methanol}$ at 1 and 5 μm scanning distances are represented in **Scheme 2**a,b, respectively.

The load-dependent frictional behavior of both homogeneous and stratified films was also studied and is reported in **Figure 4**. PAAm-0 and PAAm-1 showed contrasting behavior, in accordance with previously reported results.[14] Brushes were characterized by a very low and nearly constant friction force with increasing load (low coefficient of friction), while grafted gels showed high frictional force due to the increased dissipation of the crosslinked network. In line with the behavior of homogeneous PAAm films, the frictional properties of the stratified layers were mainly determined by the polymer architecture exposed at the interface to the solvent (i.e., brush or gel). Hence PAAm-1–0 films (blue curve) displayed friction force vs load profiles that were comparable to PAAm-0, while PAAm-0–1$_{methanol}$ showed a frictional behavior similar to that of a 'pure' gel such as PAAm-1. Interestingly, PAAm-0 and PAAm-0–1$_{water}$ presented very similar coefficients of friction (around 0.05), typical of a swollen brush.[14,31] These results

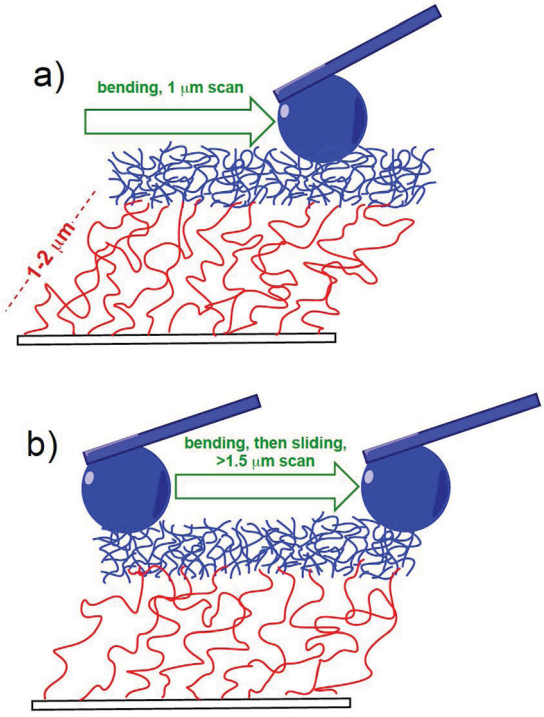

Scheme 2. Proposed sliding mechanism of PAAm-0–$1_{methanol}$ films in water with different scanning distances under same applied load. (a) Scanning distance of 1μm, in which no sliding occurs but only bending and stretching of the brush layer (b) scanning distance of 5 μm, in which after an initial bending and stretching of the brush layer, the colloidal probe begins to slide over the gel layer.

are completely consistent with the observations derived from all other characterization methods applied on these samples. The LFM investigation revealed PAAm-0 and PAAm-0–1_{water} as having very similar interfacial, brush-like properties, thus supporting the argument that when sequential polymerization was carried out in a good solvent, such as pure water, it was impossible to obtain a vertically well-defined layered brush-gel film.

Thus we conclude that the nano-tribological properties of the stratified PAAm films in aqueous environments are mainly determined by the structure of the outer layer (either a brush or a gel) at which the sliding takes place. In the case of PAAm-0–$1_{methanol}$ the inner brush structure influences friction traces via brush bending, but only in the case where static friction is predominant, i.e., at small sliding distances comparable to the extension of the underlying brush.

Combining nano-mechanical, adhesive and frictional AFM characterization methods, a comprehensive insight into the architecture and properties of stratified brush films has been gained. Focusing on the synthesis of well-defined brush-gel layered films, we have emphasized the role of solvent quality (and thus brush swelling) during sequential SIP in order to selectively confine re-initiation to the top brush-solvent interface and to avoid polymer grafting within the already synthesized layer. Our results suggested that commonly used spectroscopic methods (such as ellipsometry and FT-IR) were insufficient to reveal the structure of layered, surface-grafted polymer films. However, a comprehensive interfacial analysis based on AFM provided additional information on the film characteristics and architectures.

In conclusion, we have described the successful fabrication of stratified PAAm films with gel-brush and brush-gel structures by sequential iniferter-mediated SIP. These vertically structured films represent the first example of stratified grafted polymer layers with precisely adjustable and gradable bulk physical and interfacial properties. Their potential application as coatings with controlled surface properties and 3D architectures can find application in the development of novel interfaces for biomaterials and supports for cell adhesion. In these particular applications, the intrinsic characteristics of layered brush films mimic the graded properties of many natural interfaces. Layered brush coatings featuring well-defined characteristics could efficiently trigger a specific biological response or locally mimic the natural gradation of properties present in extra-cellular matrix (ECM) environments, coatings of biological origin or tissue surfaces. The use of sequential SIP in selective solvent environments could thus represent an effective strategy to vary the physical properties of coatings in a controlled manner obtaining graded architectures. This could be extended to different chemistries and polymerization processes suitable for a large variety of supports and applications.

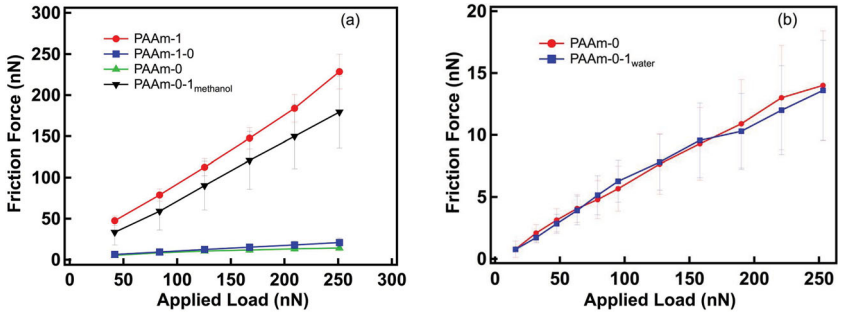

Figure 4. (a) Friction of homogeneous and stratified PAAm films measured by CPM (spring constant: 1.28 N/m, radius of silica probe: 9.1 μm, sliding distance: 5 μm, sliding speed: 10 μm/s) in water. Dry mass of polymer films on silicon substrate: PAAm-1: 148 mg/m^2, PAAm-1–0: 148–30 mg/m^2, PAAm-0: 52 mg/m^2, PAAm-0–$1_{methanol}$: 52–108 mg/m^2. (b) Friction of PAAm-0 and PAAm-0–1_{water} measured by CPM (spring constant: 0.51 N/m, radius of silica probe: 8.7 μm) in water with a sliding distance of 5 μm (sliding speed: 10 μm/s). Dry mass of polymer films on silicon substrate: PAAm-0: 31 mg/m^2, PAAm-0–1_{water}: 31–42 mg/m^2.

Experimental Section

Materials: *p*-(chloromethyl)phenyltrimethoxysilane (95%, ABCR, Germany), acrylamide (99+%, Acros Organics), *N*,*N*-methylenebis(acrylamide) (>99.0%, Fluka-Chemie AG, Switzerland), methanol (Fluka-Chemie AG, Switzerland), triethylamine (>99.5%, Sigma-Aldrich, Germany), sulfuric acid (95–97%, Sigma-Aldrich, Germany) and hydrogen peroxide (30 wt% in water, Merck, Germany) were used as received. Tetrahydrofuran (THF, 99.5% extra dry, Acros, Germany) and toluene (>99.7%, Fluka-Chemie AG, Switzerland) were freshly distilled over sodium prior to use. Sodium

N,*N*-diethyldithiocarbamate (97%, Fluka-Chemie AG, Switzerland) was recrystallized from methanol. Water was deionized with a GenPure filtration system (18.2 MΩ cm, TKA, Switzerland). The synthesis of photoiniferter, the iniferter immobilization on silicon wafer, as well as the fabrication of homogeneous poly(acrylamide) films with different crosslink degrees were carried out according to the procedure previously reported by us. In particular, the concentration of crosslinker within the films was compared to the monomer/crosslinker feed composition and a linear relationship was found.[14] The stratified PAAm films were synthesized by reinitiating the substrate covered with prefabricated homogeneous PAAm thin films in a monomer (crosslinker) medium through surface-initiated photoiniferter-mediated polymerization (SI-PIMP). For the synthesis of films with gel-brush structure (PAAm-1–0), the substrate bearing PAAm-1 gel films was placed in a flask filled with degassed methanol-free AAm aqueous solution (1 M) under an Ar atmosphere; then the UVLED irradiation was applied for a specific time, resulting in the formation of films with the targeted structure. In the case of the synthesis of the stratified brush-gel films, PAAm-0 was placed in a flask filled with either water or water-methanol mixtures (volume fraction of methanol: 75%) of monomers under an Ar atmosphere (AAm: 1 M, W_{bisAAm}:$W_{solvents}$ = 1.0%); then the reinitiation was started by applying UV irradiation for a specific time, resulting in either PAAm-0–1_{water} or PAAm-0–$1_{methanol}$, respectively. After the polymerization all the samples were rinsed copiously with Milli-Q water, immersed in water overnight, prior to further characterization. A constant UV irradiation intensity (5.5 mW cm^{-2}) was used through all synthesis processes.

Ellipsometry: The dry thicknesses of surface-grafted polymer films were determined by means of a variable-angle spectroscopic ellipsometer (VASE) (M-2000F, LOT Oriel GmbH, Darmstadt, Germany) at three different incidence angles (65°, 70°, 75°), in ambient environments with a relative humidity of 28.4%, under the assumption that the polymer has a refractive index of 1.45. The thickness was determined via the analysis of a five-layer (Si/SiO_2/Iniferter/PAAm/Ambient) model with known thicknesses and refractive indices of the Si, SiO_2 and iniferter layers (software WVASE32, LOT Oriel GmbH, Darmstadt, Germany). Ellipsometry was also conducted under liquids; however, polymeric films with brush structures were so strongly swollen in water that no refractive index contrast between polymer films and water could be detected. Therefore, swelling thicknesses of these films could not be obtained by ellipsometry.

Due to our inadequate knowledge of the location of reinitiating SI-PIMP within the initial polymeric layer, the thickness of both homogeneous and stratified PAAm films following the sequential photografting step in this study are converted to the mass gained ($\Delta\delta$) according to the equation below:[35]

$$\Delta\delta = \rho \times \Delta d \quad (1)$$

where ρ is the poly(acrylamide) density (0.8 g/cm^3)[36] and Δd is the change of thickness.

Fourier Transform Infrared Spectroscopy (FT-IR): FT-IR spectra were recorded on the dried samples in transmission mode by employing an infrared spectrometer (Bruker, IFS 66 V) equipped with a liquid-nitrogen-cooled MCT detector. A background spectrum was collected from a freshly cleaned, bare silicon wafer.

Atomic Force Microscopy (AFM): The morphologies of homogeneous and stratified PAAm films were imaged in a closed liquid cell with a Cypher™ AFM (Asylum Research, Santa Barbara, USA) in water. A triangular-shaped cantilever with a silicon nitride tip (spring constant: 0.32 N m^{-1}, model: DNP-S, Veeco, USA) was used in fluid AC mode to acquire height images over the scanning area (5 μm × 5 μm).

Colloidal Probe Microscopy (CPM): Normal-force and friction measurements between a silica microsphere and surface-grafted homogeneous and stratified polymer films were carried out in Milli-Q water using an AFM (MFP3D, Asylum Research, Santa Barbara, USA) equipped with a liquid cell. The normal spring constant of the Au-coated tipless cantilever (NSC-12, Mikromash, Estonia) was measured by the thermal-noise method[37] and the torsional spring constant was measured according to Sader's method.[38] Both normal and torsional spring constants of the cantilever were measured before attaching the colloidal microsphere. A silica microparticle (Kromasil, EKA Chemicals AB, USA) was glued with UV-curable glue (Norland Optical Adhesive 63, Norland Products, USA) to the end of the tipless cantilever by means of a home-built micromanipulator, to be further used for colloidal probe microscopy.[39]

The modulus values were estimated from the measured force-indentation curves using a Hertz fit (Asylum software, version AR12). The initial 15% to 50% of the curve was used to fit the Hertz equation. The initial (<15%) and latter part (<50%) of the force curve includes a highly repulsive regime and substrate effects, respectively, and thus were not included in the fit. The tip modulus and Poisson's ratio for the silica colloid were chosen to be 74 GPa and 0.2, respectively. The Poisson's ratio for the polymer films was approximated as 0.5.[40]

For lateral-force measurements, 10 'friction loops' along the same scan line were acquired at each load with a specific scanning rate as well as scanning distance, from which the average friction force and the standard deviation could be calculated. Both normal-force and friction measurements were repeated at three different locations on the polymer films.

The lateral-force calibration was conducted by employing the 'test-probe method'.[41] To determine the lateral sensitivity of the photo detector, a freshly cleaned silicon wafer (1 cm × 1 cm) was glued 'edge-on' to a glass slide. The smooth silicon plane was used as a 'wall' for measuring the lateral sensitivity. A test probe (cantilever glued with a silica colloidal sphere of diameter around 40 μm) was moved laterally into contact. The slope of the obtained lateral-deflection-vs-piezo-displacement curve yields the lateral sensitivity, to be used for lateral-force calibration.

Supporting Information

Supporting Information is available from the Wiley Online Library or from the author.

Acknowledgements

AL and SNR contributed equally to this work. The financial assistance of the European Science Foundation, through their Eurocores (FANAS) program is gratefully acknowledged.

Received: August 15, 2013
Revised: September 22, 2013
Published online: October 21, 2013

[1] R. A. Stockwell, J. E. Scott, *Nature* **1967**, *215*, 1376.
[2] J. C. Mackenzie, *Nature* **1969**, *222*, 881.
[3] H. D. Espinosa, A. L. Luster, F. J. Latourte, O. Y. Loh, D. Gregoire, P. D. Zavattieri, *Nat. Commun.* **2011**, *2*, 173.
[4] J. R. Stokes, In *Food Oral Processing: Fundamentals of Eating and Sensory Perception* (Eds: J. S. Chen, L. Engelen), Wiley-Blackwell, Chichester, UK **2012**, Ch. 12.
[5] J. Genzer, J. Groenewold, *Soft Matter* **2006**, *2*, 310.
[6] S. Suresh, *Science* **2001**, *292*, 2447.
[7] C. Ortiz, M. C. Boyce, *Science* **2008**, *319*, 1053.
[8] B. J. F. Bruet, J. Song, M. C. Boyce, C. Ortiz, *Nat. Mater.* **2008**, *7*, 748.
[9] S. Edmondson, V. L. Osborne, W. T. S. Huck, *Chem. Soc. Rev.* **2004**, *33*, 14.
[10] R. Barbey, L. Lavanant, D. Paripovic, N. Schüwer, C. Sugnaux, S. Tugulu, H. A. Klok, *Chem. Rev.* **2009**, *109*, 5437.

[11] M. C. LeMieux, S. Peleshanko, K. D. Anderson, V. V. Tsukruk, *Langmuir* **2007**, *23*, 265.
[12] *Polymer Surfaces and Interfaces: Characterization, Modification and Applications* (Ed: M. Stamm), Springer-Verlag, Heidelberg, Germany **2008**.
[13] E. M. Benetti, X. Sui, S. Zapotoczny, G. J. Vancso, *Adv. Funct. Mater.* **2010**, *20*, 939.
[14] A. Li, E. M. Benetti, D. Tranchida, J. N. Clasohm, H. Schönherr, N. D. Spencer, *Macromolecules* **2011**, *44*, 5344.
[15] K. Matyjaszewski, *Macromol. Rapid Commun.* **2005**, *26*, 135.
[16] Several attempts have been made to measure the swollen thickness for our studied system, using methods such as neutron scattering and ellipsometry. However, the high water content of the PAAm layer ('ghost films') did not allow a clear estimation of the swelling characteristics. Since we are aware of the swelling ratio of homogeneous PAAm films (*Q* of PAAm-0: 26, *Q* of PAAm-1: 3, in Ref. 14), a 65 nm dry PAAm-0 film has an estimated wet thickness of 1.7 µm, which is roughly in line with the reported indentation depths.
[17] M. Lemieux, D. Usov, S. Minko, M. Stamm, H. Shulha, V. V. Tsukruk, *Macromolecules* **2003**, *36*, 7244.
[18] J. X. Feng, R. T. Haasch, D. J. Dyer, *Macromolecules* **2004**, *37*, 9525.
[19] S. B. Rahane, A. T. Metters, S. M. Kilbey II, *J. Polym. Sci. A Polym. Chem.* **2010**, *48*, 1586.
[20] *Polymer Brushes: Substrates, Technologies, and Properties* (Ed: V. Mittal), CRC Press, Boca Raton, USA **2012**, Ch. 12.
[21] B. Akgun, G. Ugur, W. J. Brittain, C. F. Majkrzak, X. F. Li, J. Wang, H. M. Li, D. T. Wu, Q. Wang, M. D. Foster, *Macromolecules* **2009**, *42*, 8411.
[22] G. J. Fleer, M. A. Cohen Stuart, J. M. H. M. Scheutjens, T. Cosgrove, B. Vincent, *Polymers at Interfaces*, Chapman & Hall, London, UK **1993**.
[23] N. Spiliopoulos, A. G. Koutsioubas, D. L. Anastassopoulos, A. A. Vradis, C. Toprakcioglu, A. Menelle, G. Mountrichas, S. Pispas, *Macromolecules* **2009**, *42*, 6209.
[24] J. K. Basu, J. C. Boulliard, B. Capelle, J. Daillant, P. Guenoun, J. W. Mays, J. Yang, *Macromolecules* **2007**, *40*, 6333.
[25] A. Milchev, J. P. Wittmer, D. P. Landau, *J. Chem. Phys.* **2000**, *112*, 1606.
[26] V. A. Baulin, E. B. Zhulina, A. Halperin, *J. Chem. Phys.* **2003**, *119*, 10977.
[27] E. B. Zhulina, O. V. Borisov, V. A. Pryamitsyn, T. M. Birshtein, *Macromolecules* **1991**, *24*, 140.
[28] V. M. Amoskov, T. M. Birshtein, *Macromol. Theory Simul.* **2009**, *18*, 453.
[29] A. Li, S. N. Ramakrishna, E. S. Kooij, R. M. Espinosa-Marzal, N. D. Spencer, *Soft Matter* **2012**, *8*, 9092.
[30] *Polymer Handbook* (Eds: J. Brandrup, E. H. Immergut, E. A. Grulke, A. Abe, D. R. Bloch), 4th ed., John Wiley & Sons, New York **2005**.
[31] M. T. Müller, X. Yan, S. Lee, S. S. Perry, N. D. Spencer, *Macromolecules* **2005**, *38*, 3861.
[32] R. M. Espinosa-Marzal, R. M. Bielecki, N. D. Spencer, *Soft Matter* **2013**, *9*, 10572.
[33] M. Kwak, H. Chung, J. Choi, H. Kwon, J. Kim, D. Han, C. Park, S. Lee, C. Lee, S. Cha, *Mol. Cryst. Liq. Cryst.* **2009**, *507*, 129.
[34] P. C. Nalam, S. N. Ramakrishna, R. M. Espinosa-Marzal, N. D. Spencer, *Langmuir* **2013**, *29*, 10149.
[35] H. N. Zhang, J. Rühe, *Macromolecules* **2005**, *38*, 10743.
[36] Material Safety Data Sheet, Polyacrylamide, Carl Roth, **2012**.
[37] H. J. Butt, M. Jaschke, *Nanotechnology* **1995**, *6*, 1.
[38] C. P. Green, H. Lioe, J. P. Cleveland, R. Proksch, P. Mulvaney, J. E. Sader, *Rev. Sci. Instrum.* **2004**, *75*, 1988.
[39] W. A. Ducker, T. J. Senden, R. M. Pashley, *Nature* **1991**, *353*, 239.
[40] A. Li, S. N. Ramakrishna, T. Schwarz, E. M. Benetti, N. D. Spencer, *ACS Appl. Mater. Interfaces* **2013**, *5*, 4913.
[41] R. J. Cannara, M. Eglin, R. W. Carpick, *Rev. Sci. Instrum.* **2006**, *77*, 053701.